# A MULTI-VIEW DIMENSIONALITY REDUCTION ALGORITHM BASED ON SMOOTH REPRESENTATION MODEL

A PREPRINT

**Haohao Li**
School of Mathematical Sciences
Dalian University of Technology
Dalian District of Ganjingzi City Road 2
hhl820@mail.dlut.edu.cn

**Huibing Wang**
Information Science And Technology College
Dalian Maritime University
Dalian Linghai Road1,

May 15, 2022

**ABSTRACT**

Over the past few decades, we have witnessed a large family of algorithms that have been designed to provide different solutions to the problem of dimensionality reduction (DR). The DR is an essential tool to excavate the important information from the high-dimensional data by mapping the data to a low-dimensional subspace. Furthermore, for the diversity of varied high-dimensional data, the multi-view features can be utilized for improving the learning performance. However, many DR methods fail to integrating multiple views. Although the features from different views are extracted by different manners, they are utilized to describe the same sample, which implies that they are highly related. Therefore, how to learn the subspace for high-dimensional features by utilizing the consistency and complementary properties of multi-view features is important in the present. In this paper, we propose an effective multi-view dimensionality reduction algorithm named Multi-view Smooth Preserve Projection. Firstly, we construct a single view DR method named Smooth Preserve Projection based on the Smooth Representation model. The proposed method aims to find a subspace for the high-dimensional data, in which the smooth reconstructive weights are preserved as much as possible. Then, we extend it to a multi-view version in which we exploits Hilbert-Schmidt Independence Criterion to jointly learn one common subspace for all views. A plenty of experiments on multi-view datasets show the excellent performance of the proposed method.

***K*eywords** Multi-view Learning · Dimensionality Reduction · Smooth Representation

## 1 Introduction

With the development of information acquirement techniques, the features of samples are usually collected from different tools [1–3], which generates the multi-view features in various applications. Features from multiple views can describe the properties of samples more comprehensively than one from single view.For instance, in computer vision domain, images can be depicted with different descriptors, such as Local Binary Patterns (LBP), Histograms of Oriented Gradients (HOG) and Gist [4], which can be regarded as .three-view feature. How to make good use of the information of features from multiple views for improving performance is the most important purpose of multi-view learning.

In many fields, such as face recognition, text categorization and information retrieval, most of the extracted features locate in a high-dimensional space, which usually leads to the curse-of-dimensionality. To deal with this problem, a variety of DR techniques are developed [5–13]. Principal Component Analysis (PCA) [5] might be one of the most popular unsupervised dimensionality reduction algorithms. PCA performs dimensionality reduction by projecting original data to the linear subspace spanned by the leading eigenvectors of covariance matrix of the data. LDA [6] is a supervised linear DR method which makes use of label information. It constructs the linear projection by maximizing the generalized Rayleigh quotient function of between-class scatter and within-class scatter, which has more discriminative

ability than PCA. Although they are simple and convenient, PCA and LDA may fail to discover local structures of data. Different from PCA and LDA which aims at preserving the global Euclidean structure, Locality Preserving Projection (LPP) [7] and Neighborhood Preserving Embedding (NPE) [8] consider the local manifold structure. They represent each data point as a linear combination of other data points and the combination coefficients are specified in a weight matrix, which is constructed to describe the relationship between the data points. Marginal Fisher Analysis (MFA) [9] and Sparsity Preserving Projections (SPP) [14] are local methods which construct low-dimensional subspaces based on different graph of data points. Unlike the linear DR methods above, manifold learning is a technique for nonlinear DR. A variety of manifold learning methods have been developed to discover the nonlinear manifold structure of the data, such as Locally Linear Embedding (LLE) [15], Isomap and Laplacian Eigenmaps (LE) [16], etc. However, most traditional DR methods cannot integrate compatible and complementary information from multi-view features when constructing low-dimensional subspace.

Multi-view learning aims to learn one function for each view and jointly optimizes all views' functions to improve the performance. Multi-view DR is an important branch of multi-view learning [17–31], which seeks one low-dimensional common subspace for representing multi-view features. Canonical correlation analysis (CCA) [17] is a typical multi-view DR method, which can cope with two-view case. CCA aims to find two linear transformations for every view to maximize the correlation between two-view features. Then the multi-view CCA is proposed to extend the traditional CCA to a multi-view case. Following this, Multi-view Discriminant Analysis (MvDA) [18] is an extension of traditional LDA. MvDA aims to find a common discriminant subspace by jointly learning linear projections for all views, while introducing the Fisher criteria in parallel. Xia et al. [19] propose a multi-view spectral embedding (MSE) which encodes different features in different ways. In particular, MSE obtains a low dimensional embedding wherein the distribution of each view is sufficiently smooth, by exploiting the complementary property of different views. Ding et al. [20] propose a multi-view subspace learning algorithm which seeks one common low-rank linear projection to mitigate the semantic gap among various views. The projection catches compatible intrinsic information across features from all views. Yu et al. [32] propose a new multi-view DR method named pairwise constraints based multiview subspace learning (PC-MSL). PC-MSL constructs the low-dimensional subspace by considering both intraclass and interclass geometries, in which the discrimination is effectively preserved.

In this paper, we focus on multi-view DR algorithm. As discussed above, dimension reduction is a necessary tool for analyzing the samples with high dimension. Many researchers have shown that most of the existing DR methods can be unified under graph embedding framework based on the kernel view, where the affinity weight matrix for constructing the graph plays a key role. To get more effective affinity weight matrix, a great number of researches apply self-representation idea to construct it. One of the most famous self-representation method is Sparse Subspace Clustering (SSC) which encourages sparsity for data selection and SPP [14] is proposed based on it. SPP exploits affinity matrix which is calculated by Sparse Representation (SR) as the sparse reconstructive weights and then seeks a linear subspace in which the weights are preserved. However, if samples from the same class are highly correlated, SR will generally select a single representative at random, and ignore other correlated samples. This leads to that the affinity matrix misses data correlation information. Hence SPP may obtain unsatisfactory performance. To deal with this problem, the concept of grouping effect is proposed by Lu et al. [33, 34]. The grouping effect is important for stability of affinity matrix, which means that when the data points are close to each other, the representation coefficients of them are also close to each other and provides the effectiveness for some representation based method. Then, Hu et al. [35] introduce the enforced grouping effect (EGE) conditions to facilitate the analysis of grouping effect and propose an effective subspace clustering method named Smooth Representation (SMR) model, which shows many excellent results in some datasets. Motivated by SMR model, we propose a new effective DR algorithm named Smooth Preserve Projection (SmPP). First, we calculate the affinity matrix as the reconstructive weights based on a modified SMR model first. The affinity matrix can group the correlated data whithin cluster. Then, similar to the SPP, we construct subspace where the weights are preserved as much as possible. With the wide applications of multi-view data, many multi-view methods are developed based on single view one and always obtain the better performance than the their single view versions. Therefore, in this paper, we extend the SmPP to a multi-view DR method named Multi-view SmPP (MSmPP) by jointly learning the subspace for features from each view. For the features from same view, MSmPP fully exploited the reconstructive relationships them. Furthermore, since multiple views may have different impacts on the algorithm, MSmPP can automatically assign different weight factors to multiple views according their contributions. Then, MSmPP forces all views to help each other to improve its discriminative ability based on a co-regularization scheme. The contributions of our work are summarized as follows:

1. We propose a novel DR approach named SmPP which shares some advantages of both LPP and other linear DR methods. SmPP tends to seek the discriminative projection since the smooth representation usually have much large gap between the within-class and the between-class distance.
2. We extend SmPP to Multi-view SmPP (MSmPP), which can combine compatible and complementary information from multiple views features. In MSmPP algorithm, each subspace for one view is constructed by

considering the weight from all views, which can be complemented by ones from the other views and lead to a more excellent subspace.

The rest of this paper is organized as follows: in section 2, we introduce some related approaches and a basis method of multi-view learning. In section 3, we describe the details of constructing SmPP. In section 4 we extend SmPP to a multi-view framework and illustrate the optimization procedure. In section 5 experimental results are shown. Section 6 concludes this paper.

## 2 Related Work

In this section, we first review a single view linear DR method. Then, we introduce a multi-view DR algorithm named Multi-view Canonical Correlation Analysis (MCCA), which is a typical multi-view DR method. Some multi-view DR algorithms are developed by involving MCCA or other space transformation methods.

### 2.1 Linear unsupervised dimensionality reduction

Neighborhood preserving embedding (NPE) is a popular linear DR method, which aims to preserving the local neighborhood structure of the data. Given a set of data points $\{\boldsymbol{x}_i\}_{i=1}^n$, the algorithmic procedure of NPE is stated below:

(1) Constructing a weight matrix $\boldsymbol{W}$ by minimizing the following objective function:

$$\min_{\boldsymbol{W}} \quad \sum_i || \boldsymbol{x}_i - \sum_j w_{ij} \boldsymbol{x}_j ||^2 \quad s.t. \quad \sum_j w_{ij} = 1, \tag{1}$$

where $\boldsymbol{W} = (w_{ij})$ is the reconstructive matrix.

(2) Finding the linear projection that preserves the local neighborhood information by optimizing the objective function as:

$$\min_{\boldsymbol{V}} \quad \sum_i || \boldsymbol{V}^T \boldsymbol{x}_i - \sum_j w_{ij} \boldsymbol{V}^T \boldsymbol{x}_j ||^2, \tag{2}$$

where the $w_{ij}$ is the optimal solution of Equation 1. In order to avoid degenerate solutions, NPE imposes a constrain $\boldsymbol{V}^T \boldsymbol{X} \boldsymbol{X}^T \boldsymbol{V} = \boldsymbol{I}$, and the objective function can be reformulated as:

$$\min_{\boldsymbol{V}} \quad \boldsymbol{V}^T \boldsymbol{X} \boldsymbol{P} \boldsymbol{X}^T \boldsymbol{V} \quad s.t. \quad \boldsymbol{V}^T \boldsymbol{X} \boldsymbol{X}^T \boldsymbol{V} = \boldsymbol{I}, \tag{3}$$

where $\boldsymbol{P} = (\boldsymbol{I} - \boldsymbol{W})^T (\boldsymbol{I} - \boldsymbol{W})$. The optimization problem boils down to a generalized eigenvalue problem.

### 2.2 Multi-view Canonical Correlation Analysis

Multi-view Canonical Correlation Analysis (MCCA) is a generalization of CCA for multi-view scenario. Given a dataset consists of $N$ samples with $v$th view features being $\boldsymbol{X}^{(v)}$. MCCA aims to find a set of linear transformation that project samples from multiple views $\{\boldsymbol{X}^{(1)}, \boldsymbol{X}^{(2)}, ..., \boldsymbol{X}^{(m)}\}$ to one common subspace by maximizing the sum of correlation between the low-dimensional embedding of any two views:

$$\begin{aligned} &\max_{\boldsymbol{W}_1, \boldsymbol{W}_2, ..., \boldsymbol{W}_m} \quad \sum_{i<j} \boldsymbol{W}_i^T \boldsymbol{X}^{(i)} \boldsymbol{X}^{(j)} \boldsymbol{W}_j \\ &s.t. \quad \boldsymbol{W}_i^T \boldsymbol{X}^{(i)} \boldsymbol{X}^{(i)} \boldsymbol{W}_i = \boldsymbol{I}, \quad i = 1, 2, ..., m, \end{aligned} \tag{4}$$

where $\boldsymbol{X}^{(i)} \in \mathbb{R}^{d_i \times N}$ is data matrix of $i$th view feature which locates in $d_i$-dimensional space, $\boldsymbol{W}_i$ is the linear projection for $i$th view feature. The Equation 4 can be solved by alternation method to update every linear transformation.

## 3 Smooth Preserving Projection

In this section, we introduce a novel single-view DR method named Smooth Preserving Projection (SmPP). Since DR is mainly characterized by specify affinity weight matrix of data, we construct the matrix based on a modified SMR model

framework. Then we can calculate the projection for the data points based on the weight matrix. For completeness, we briefly review the concept of self-representation model and grouping effect. Given a set of data points $\{\boldsymbol{x}_i\}_{i=1}^n$, we use $\boldsymbol{X} = [\boldsymbol{x}_1, \boldsymbol{x}_2, ..., \boldsymbol{x}_n]$ to express the data matrix with each column being a sample vector. Most of representation models can be formulated as follows:

$$\begin{aligned} \min_{\mathbf{Z}} \quad & \eta||\boldsymbol{X} - \boldsymbol{X}\boldsymbol{Z}||_l + \Omega(\boldsymbol{X}, \boldsymbol{Z}), \\ s.t. \quad & \boldsymbol{Z} \in C, \end{aligned} \tag{5}$$

where $\boldsymbol{Z}$ is the self-representation matrix, $\Omega(\boldsymbol{X}, \boldsymbol{Z})$ and $C$ are regularizer and constraint set on $\boldsymbol{Z}$, respectively, and $\eta > 0$ is a trade-off parameter. The self-representation matrix $\boldsymbol{Z} = [\boldsymbol{z}_1, \boldsymbol{z}_2, ..., \boldsymbol{z}_n] \in \mathbb{R}^{n \times n}$ has grouping effect if $||\boldsymbol{x}_i - \boldsymbol{x}_j||_2 \to 0 \Rightarrow ||\boldsymbol{z}_i - \boldsymbol{z}_j||_2 \to 0, \forall i \neq j$.

We aim to reconstruct each sample using other samples which are close to it. Hence, we construct the model to seek the reconstructive matrix through the following modified SMR model:

$$\begin{aligned} \min_{\mathbf{Z}} \quad & \eta||\boldsymbol{X} - \boldsymbol{X}\boldsymbol{Z}||_F^2 + Tr(\boldsymbol{Z}\hat{\boldsymbol{L}}\boldsymbol{Z}^T), \\ s.t. \quad & \mathbf{1}^T\boldsymbol{z}_i = 1, \quad i = 1, 2, ..., n, \end{aligned} \tag{6}$$

where $\hat{\boldsymbol{L}} = \boldsymbol{L} + \epsilon\boldsymbol{I}$, and $\boldsymbol{L}$ is the Laplace matrix of $\boldsymbol{X}$. The term $\epsilon\boldsymbol{I}$ is utilized to enforce the $\hat{\boldsymbol{L}}$ to be strictly positive definite and $0 < \epsilon \ll 1$. The regularization term in Equation 6 can be expanded as follow:

$$Tr(\boldsymbol{Z}\hat{\boldsymbol{L}}\boldsymbol{Z}^T) = \epsilon||\boldsymbol{Z}||_F^2 + \frac{1}{2}\sum_{i=1}^n\sum_{j=1}^n w_{ij}||\boldsymbol{z}_i - \boldsymbol{z}_j||_2^2, \tag{7}$$

where $\boldsymbol{W} = (w_{ij})$ is weight matrix that measures the distance between the data points, and $\boldsymbol{L} = \boldsymbol{D} - \boldsymbol{W}$ is the Laplace matrix with $\boldsymbol{D} = diag\{d_1, d_2, ..., d_n\}, d_i = \sum_{j=1}^n w_{ij}$. Now we give some insights of the reconstructive matrix $\boldsymbol{Z}$ based on the viewpoint of optimization. The first term in Equation 6 which encodes the subspace structure of data points penalizes the reconstruction error. Minimizing the regularization term can naturally enforce the grouping effect by the affinity of samples in this model. Therefore, seconde term (regularization term) in Equation 6 is exploited to penalize the discontinuities in the representation coefficients. With this term, the representation will be stable. Furthermore, spatially close data points may help each other to prevent over-fitting in reconstruction the samples.

However, with this constraint set on $\boldsymbol{Z}$ Equation 6 will not satisfy the EGE conditions [35]. Therefore, we relax the restriction on $\boldsymbol{Z}$ and reformulate the Equation 6 as follows:

$$\min_{\mathbf{Z}} \quad \eta||\boldsymbol{X} - \boldsymbol{X}\boldsymbol{Z}||_F^2 + \eta\sum_{i=1}^n(1 - \boldsymbol{1}^T\boldsymbol{z}_i)^2 + Tr(\boldsymbol{Z}\hat{\boldsymbol{L}}\boldsymbol{Z}^T). \tag{8}$$

Minimizing Equation 8 makes $\boldsymbol{1}^T\boldsymbol{z}_i \to 1$. Then, for the optimal solution $\boldsymbol{Z}^* = [\boldsymbol{z}_1^*, \boldsymbol{z}_2^*, ..., \boldsymbol{z}_n^*] \in \mathbb{R}^{n \times n}$, we normalize the $\boldsymbol{Z}^*$ by $\bar{\boldsymbol{z}_i^*} = \boldsymbol{z}_i^* / \sum_{j=1}^n z_{ij}^*$. The $\bar{\boldsymbol{Z}^*} = [\bar{\boldsymbol{z}_1^*}, \bar{\boldsymbol{z}_2^*}, ..., \bar{\boldsymbol{z}_n^*}]$ is treated as the affine weight matrix of data point in our method. The Appendix shows the optimization of Equation 8 and the proof that affine weight matrix $\boldsymbol{Z}^*$ has grouping effect.

We utilize $\boldsymbol{Z}$ to represent the regularized optimal solution of Equation 8 for convenience. By the above design, the weight matrix contains grouping effect and natural discriminating information, which ensures that the reconstruction coefficients of the highly corrected data which are usually from the same subspace can be close. Hence we expect that the desirable characteristics in the original high-dimensional space can be preserved in the low-dimensional projective subspace. Similar to LLE and NPE, we construct the following objective function, which seeks projections to preserve the weight matrix $\boldsymbol{Z}$.

$$\begin{aligned} \min_{\boldsymbol{v}} \quad & ||\boldsymbol{v}^T\boldsymbol{X} - \boldsymbol{v}^T\boldsymbol{X}\boldsymbol{Z}||^2 \\ & = \boldsymbol{v}^T\boldsymbol{X}(\boldsymbol{I} - \boldsymbol{Z} - \boldsymbol{Z}^T + \boldsymbol{Z}^T\boldsymbol{Z})\boldsymbol{X}^T\boldsymbol{v}, \end{aligned} \tag{9}$$

where $\boldsymbol{Z} \in \mathbb{R}^{n \times n}$ is the reconstructive weights matrix. In order to avoid degenerate solutions, we constrains $\boldsymbol{v}^T\boldsymbol{X}\boldsymbol{X}^T\boldsymbol{v} = 1$. Then, we reformulate the Equation 9 to get a compact expression as:

$$\begin{aligned} \max_{\boldsymbol{v}} \quad & \boldsymbol{v}^T\boldsymbol{X}\boldsymbol{P}\boldsymbol{X}^T\boldsymbol{v} \\ s.t. \quad & \boldsymbol{v}^T\boldsymbol{X}\boldsymbol{X}^T\boldsymbol{v} = 1, \end{aligned} \tag{10}$$

where $\boldsymbol{P} = \boldsymbol{Z} + \boldsymbol{Z}^T - \boldsymbol{Z}^T\boldsymbol{Z}$. The optimal $\boldsymbol{v}$'s are the eigenvectors corresponding to the largest $d$ eigenvalues of generalized eigenvalue decomposition problem:

$$\boldsymbol{X}\boldsymbol{P}\boldsymbol{X}^T\boldsymbol{v} = \lambda\boldsymbol{X}\boldsymbol{X}^T\boldsymbol{v}. \tag{11}$$

Let $\boldsymbol{V} = [\boldsymbol{v}_1, \boldsymbol{v}_2, ..., \boldsymbol{v}_d]$ represent the $d$ eigenvalues. And the low-dimensional representation of data points $\boldsymbol{X}$ can be expressed in the optimal subspace spanned by $\{\boldsymbol{v}_1, \boldsymbol{v}_2, ..., \boldsymbol{v}_d\}$ as:

$$\boldsymbol{Y} = [\boldsymbol{y}_1, \boldsymbol{y}_2, ..., \boldsymbol{y}_n] = \boldsymbol{V}^T\boldsymbol{X} \in \mathbb{R}^{d \times n}. \tag{12}$$

# 4 Multi-view Smooth Preserving Projection

In this section, we introduce the procedure of extending the single view SmPP to Multi-view SmPP (MSmPP). In section 4.1, we show the details of construction of MSmPP which finds one common low-dimensional subspace over all views simultaneously by integrating compatible and complementary information from multi-view features. In section 4.2, the optimization procedure of MSmPP is demonstrated.

## 4.1 MSmPP with co-regularization

MSmPP aims to fully utilize multi-view features and construct one common subspace for all views. However, different view features locate in different dimensional spaces, which causes great challenges to MSmPP. Therefore, we exploit the kernel techniques to eliminate the influence of the different dimensions of multi-view features. Meanwhile, MSmPP adopts a self-weighted learning trick to assign different factors to these views according to their contributions. At last, the co-regularization is used to make sure that data from multi-view features are consistent. We introduce the details of constructing MSmPP in the rest of this section.

Given $n$ samples with $m$ representations, i.e., a set of matrix $\boldsymbol{X} = \{\boldsymbol{X}^{(i)} \in \mathbb{R}^{d_i \times n}\}_{i=1}^{m}$, where $\boldsymbol{X}^{(i)} = [\boldsymbol{x}_1^{(i)}, \boldsymbol{x}_2^{(i)}, ..., \boldsymbol{x}_n^{(i)}]$ is $i$-th view feature matrix with each column being a sample feature vector. For $\mathbf{X}^{(i)}$, MSmPP first maps all the $x_j^{(i)}$ into kernel space by utilizing a kernel function $\phi$ as: $\phi(\boldsymbol{x}_j^{(i)})$. Then, $\boldsymbol{X}_\phi^{(i)} = [\phi(\boldsymbol{x}_1^{(i)}), \phi(\boldsymbol{x}_2^{(i)}), ..., \phi(\boldsymbol{x}_n^{(i)}))]$ represents the features which have been mapped into the kernel space. For the $i$th view, SmPP can be extended by kernel methods as:

$$\max_{\boldsymbol{v}_\phi^{(i)}} \quad (\boldsymbol{v}_\phi^{(i)})^T \boldsymbol{X}_\phi^{(i)} \boldsymbol{P}^{(i)} (\boldsymbol{X}_\phi^{(i)})^T \boldsymbol{v}_\phi^{(i)} \quad s.t. \quad (\boldsymbol{v}_\phi^{(i)})^T \boldsymbol{X}_\phi^{(i)} (\boldsymbol{X}_\phi^{(i)})^T \boldsymbol{v}_\phi^{(i)} = 1 \tag{13}$$

where $\boldsymbol{P}^{(i)} = \boldsymbol{Z}^{(i)} + (\boldsymbol{Z}^{(i)})^T - (\boldsymbol{Z}^{(i)})^T \boldsymbol{Z}^{(i)}$. The optimal $\boldsymbol{v}_\phi^{(i)}$ is a projection in the kernel space which can preserve the smooth reconstructive weights for $i$th view. Similar to Kernel PCA [36], we can formulate the $\boldsymbol{v}_\phi^{(i)}$ as $\boldsymbol{v}_\phi^{(i)} = \boldsymbol{X}_\phi^{(i)} \boldsymbol{u}^{(i)}$, where $\boldsymbol{u}^{(i)} = [\boldsymbol{u}_1^{(i)}, \boldsymbol{u}_2^{(i)}, ..., \boldsymbol{u}_n^{(i)}]^T$ is the representation coefficient. Then the Equation 13 can be reformulated as:

$$\max_{\boldsymbol{u}^{(i)}} \quad (\boldsymbol{u}^{(i)})^T \boldsymbol{K}^{(i)} \boldsymbol{P}^{(i)} \boldsymbol{K}^{(i)} \boldsymbol{u}^{(i)} \quad s.t. \quad (\boldsymbol{u}^{(i)})^T \boldsymbol{K}^{(i)} \boldsymbol{K}^{(i)} \boldsymbol{u}^{(i)} = 1 \tag{14}$$

where $\boldsymbol{K}^{(i)} = (\boldsymbol{X}_\phi^{(i)})^T \boldsymbol{X}_\phi^{(i)} \in \mathbb{R}^{n \times n}$ is the kernel matrix. The optimal solution is the eigenvectors corresponding to the largest $d$ eigenvalues of generalized eigenvalue decomposition problem as:

$$\boldsymbol{K}^{(i)} \boldsymbol{P}^{(i)} \boldsymbol{K}^{(i)} \boldsymbol{u}^{(i)} = \boldsymbol{K}^{(i)} \boldsymbol{K}^{(i)} \boldsymbol{u}^{(i)} \tag{15}$$

Then, we can obtain the optimal subspace by the objective function as:

$$\max_{\boldsymbol{U}^{(i)}} \quad Tr((\boldsymbol{U}^{(i)})^T \boldsymbol{K}^{(i)} \boldsymbol{P}^{(i)} \boldsymbol{K}^{(i)} \boldsymbol{U}^{(i)}) \quad s.t. \quad (\boldsymbol{U}^{(i)})^T \boldsymbol{K}^{(i)} \boldsymbol{K}^{(i)} \boldsymbol{U}^{(i)} = \boldsymbol{I} \tag{16}$$

The low-dimensional representation of $\boldsymbol{X}^{(i)}$ can be expressed as follows:

$$\boldsymbol{Y}^{(i)} = (\boldsymbol{X}_\phi^{(i)} \boldsymbol{U}^{(i)})^T \boldsymbol{X}_\phi^{(i)} = (\boldsymbol{U}^{(i)})^T \boldsymbol{K}^i \tag{17}$$

Then, in order to compute the projections which preserves the reconstruction weight as much as possible for each view, we need to maximize the sum of Equation 16. Accordingly, we can get following objective function:

$$\max_{\mathcal{U}} \sum_{i=1}^{m} \quad Tr((\boldsymbol{U}^{(i)})^T \boldsymbol{K}^{(i)} \boldsymbol{P}^{(i)} \boldsymbol{K}^{(i)} \boldsymbol{U}^{(i)}) \quad s.t. \quad (\boldsymbol{U}^{(i)})^T \boldsymbol{K}^{(i)} \boldsymbol{K}^{(i)} \boldsymbol{U}^{(i)} = \boldsymbol{I} \tag{18}$$

where $\mathcal{U} = \{\boldsymbol{U}^{(1)}, \boldsymbol{U}^{(2)}, ..., \boldsymbol{U}^{(m)}\}$ represents the set of the representation coefficient of all views.

Because the different property of multiple views, the views may have different contributions to constructing the low-dimensional representations in Equation 18. To better explore the complementary property of different views and treat them discriminatively based on their contributions, we impose a set of nonnegative weights $\boldsymbol{\alpha} = [\alpha_1, \alpha_2, ..., \alpha_m]$ on different views independently. The the weighting factors to these views can be learned automatically learned automatically. Therefor, we get the following maximization problem for MSmPP:

$$\begin{aligned} &\max_{\boldsymbol{\alpha}, \mathcal{U}} \sum_{i=1}^{m} \quad \alpha_i^r Tr((\boldsymbol{U}^{(i)})^T \boldsymbol{K}^{(i)} \boldsymbol{P}^{(i)} \boldsymbol{K}^{(i)} \boldsymbol{U}^{(i)}) \\ &s.t. \quad (\boldsymbol{U}^{(i)})^T \boldsymbol{K}^{(i)} \boldsymbol{K}^{(i)} \boldsymbol{U}^{(i)} = \boldsymbol{I} \quad i = 1, 2, ...m \end{aligned} \tag{19}$$

Based on the above analysis, we can explore multi-view features located in different dimensional spaces directly in our MSmPP with kernel method. Since the multi-view features are extracted from the same sample by different means, in MSmPP, we assume that the low-dimensional representations of multi-view features in true underlying subspace would be similar across all views. This assumption means that the coefficient vectors $\boldsymbol{U}^{(i)}$ and $\boldsymbol{U}^{(j)}$ of a view pair $(i, j)$ should have high pairwise similarity. Therefore, we enforce features from each view to be more dependent and utilize the Hilbert-Schmidt Independence Criterion (HSIC) to measures the dependence between two views. We can maximize HSIC of two view features to enhance the dependence between them. We propose the following version of HSIC in our algorithm as a measurement of dependence between two views:

$$\text{HSIC}(\boldsymbol{Y}^{(i)}, \boldsymbol{Y}^{(l)}) = (N-1)^2 Tr(\boldsymbol{K}_{\boldsymbol{Y}^{(i)}} \boldsymbol{H} \boldsymbol{K}_{\boldsymbol{Y}^{(l)}} \boldsymbol{H}), \tag{20}$$

where $\boldsymbol{Y}^{(i)}$ is the low-dimensional representation of $\boldsymbol{X}^{(i)}$ and can be expressed as:

$$\boldsymbol{Y}^{(i)} = (\boldsymbol{X}_{\phi}^{(i)} \boldsymbol{U}^{(i)})^T \boldsymbol{X}_{\phi}^{(i)} = (\boldsymbol{U}^{(i)})^T \boldsymbol{K}^{(i)} \in \mathbb{R}^{d \times N}.$$

And $\boldsymbol{H} = (h_{jk}), h_{jk} = \delta_{jk} - \frac{1}{N}$. Maximizing Equation 20 guarantees these features to be dependent, which can share complementary information to help MSmPP to construct the subspace for every view features. For the kernel $\boldsymbol{K}_{\boldsymbol{Y}^{(i)}}$ we choose the inner product function, i.e., $\boldsymbol{K}_{\boldsymbol{Y}^{(i)}} = (\boldsymbol{Y}^{(i)})^T \boldsymbol{Y}^{(i)}$. Substituting this and the expression of $\boldsymbol{Y}^{(i)}$ in Equation 20, we can get following formulation:

$$\text{HSIC}(\boldsymbol{Y}^{(i)}, \boldsymbol{Y}^{(l)}) = (N-1)^2 Tr((\boldsymbol{U}^{(i)})^T \boldsymbol{K}^{(i)} \boldsymbol{G}^{(l)} (\boldsymbol{K}^{(i)})^T \boldsymbol{U}^{(i)}), \tag{21}$$

where $\boldsymbol{G}^{(l)} = \boldsymbol{H}(\boldsymbol{K}^{(l)})^T \boldsymbol{U}^{(l)} (\boldsymbol{U}^{(l)})^T \boldsymbol{K}^{(l)} \boldsymbol{H}$.

Maximizing HSIC enforces that the all the view pair should have high pairwise similarity, which can help MSmPP to construct a common subspace by exploring compatible and complementary information from multi-view features. Therefore, combining this term, we get the following co-regularization maximization problem as:

$$\begin{aligned} \max_{\boldsymbol{\alpha}, \mathcal{U}} \quad & \sum_{i=1}^{m} \alpha_i^r Tr((\boldsymbol{U}^{(i)})^T \boldsymbol{K}^{(i)} \boldsymbol{P}^{(i)} \boldsymbol{K}^{(i)} \boldsymbol{U}^{(i)}) + \\ & \sum_{i \neq l} \beta(\alpha_i^r + \alpha_l^r)(N-1)^2 Tr((\boldsymbol{U}^{(i)})^T \boldsymbol{K}^{(i)} \boldsymbol{G}^{(l)} (\boldsymbol{K}^{(i)})^T \boldsymbol{U}^{(i)}) \\ s.t. \quad & (\boldsymbol{U}^{(i)})^T \boldsymbol{K}^{(i)} \boldsymbol{K}^{(i)} \boldsymbol{U}^{(i)} = \boldsymbol{I} \quad i = 1, 2, ...m \quad \sum_{v=1}^{m} \alpha_v = 1, \end{aligned} \tag{22}$$

where $\beta > 0$ is the regularization parameter that controls the trade-off between two terms of Equation 22. The parameter $r$ is set to $r > 1$. Since, in this condition, each view has a particular contribution to finding the final low-dimensional space (Because with the condition $r > 1$, $\sum_{i=1}^{m} \alpha_i^r$ achieves its minimum when $\alpha_i = 1/m$ with respect to $\sum_{i=1}^{m} \alpha_i = 1, \alpha_i > 0$).

### 4.2 Optimization of MSmPP

In this section, we introduce the optimization of Equation 22. To the best of our knowledge, optimizing $\boldsymbol{\alpha}$, $\boldsymbol{U}^{(i)}$ directly is a tough task. Therefore, in this paper, we derive an alternating optimization strategy to obtain an local optimal solution. The alternating optimization iteratively updates $\boldsymbol{U}^{(i)}$ and $\boldsymbol{\alpha}$ in an alternating fashion.

First, we fix $\boldsymbol{U}^{(i)}$ for all views to update $\boldsymbol{\alpha}$. By using a Lagrange multiplier $\lambda$ to take the constraint $\sum_{v=1}^{m} \alpha_v = 1$ into consideration, we get the Lagrange function as:

$$\begin{aligned} \mathcal{L}(\boldsymbol{\alpha}, \lambda) = & \sum_{i=1}^{m} \alpha_i^r Tr((\boldsymbol{U}^{(i)})^T \boldsymbol{K}^{(i)} \boldsymbol{P}^{(i)} \boldsymbol{K}^{(i)} \boldsymbol{U}^{(i)}) + \\ & \sum_{i \neq l} \beta(\alpha_i^r + \alpha_l^r)(N-1)^2 Tr((\boldsymbol{U}^{(i)})^T \boldsymbol{K}^{(i)} \boldsymbol{G}^{(l)} (\boldsymbol{K}^{(i)})^T \boldsymbol{U}^{(i)}) - \lambda(\sum_{i=1}^{m} \alpha_i - 1) \\ & = \mathcal{J}(\boldsymbol{\alpha}) - \lambda(\sum_{i=1}^{m} \alpha_i - 1) \end{aligned} \tag{23}$$

By setting the derivative of $\mathcal{L}$ with respect to $\alpha_v$ and $\lambda$ to 0, we can obtain:

$$\begin{cases} \dfrac{\partial \mathcal{L}(\boldsymbol{\alpha}, \lambda)}{\partial \alpha_i} = \dfrac{\partial \mathcal{J}(\boldsymbol{\alpha}, \lambda)}{\partial \alpha_i} - \lambda = 0 \\ \dfrac{\partial \mathcal{L}(\boldsymbol{\alpha}, \lambda)}{\partial \lambda} = \sum\limits_{i=1}^{m} \alpha_i - 1 = 0 \end{cases} \tag{24}$$

where

$$\begin{aligned} \frac{\partial \mathcal{J}(\boldsymbol{\alpha}, \lambda)}{\partial \alpha_i} &= r\alpha_i^{r-1}\{Tr((\boldsymbol{U}^{(i)})^T \boldsymbol{K}^{(i)} \boldsymbol{P}^{(i)} \boldsymbol{K}^{(i)} \boldsymbol{U}^{(i)}) \\ &+ \sum_{i \neq l} \beta(N-1)^2 Tr((\boldsymbol{U}^{(i)})^T \boldsymbol{K}^{(i)} \boldsymbol{G}^{(l)} (\boldsymbol{K}^{(i)})^T \boldsymbol{U}^{(i)}). \end{aligned} \tag{25}$$

We set

$$\mathcal{K}^i = \boldsymbol{K}^{(i)} \boldsymbol{P}^{(i)} \boldsymbol{K}^{(i)} + \sum_{\substack{l \\ i \neq l}} \beta(N-1)^2 \boldsymbol{K}^{(i)} \boldsymbol{G}^{(l)} (\boldsymbol{K}^{(i)})^T.$$

Then the $\frac{\partial \mathcal{J}(\boldsymbol{\alpha}, \lambda)}{\partial \alpha_i}$ can be rewrite as:

$$\frac{\partial \mathcal{J}(\boldsymbol{\alpha}, \lambda)}{\partial \alpha_i} = r\alpha_i^{r-1} Tr((\boldsymbol{U}^{(i)})^T \mathcal{K}^i \boldsymbol{U}^{(i)})$$

Therefore, $\alpha_v$ can be obtained as:

$$\alpha_i = \frac{(1/Tr((\boldsymbol{U}^{(i)})^T \mathcal{K}^i \boldsymbol{U}^{(i)}))^{1/(r-1)}}{\sum_{l=1}^{m} (1/Tr((\boldsymbol{U}^{(l)})^T \mathcal{K}^l \boldsymbol{U}^{(l)}))^{1/(r-1)}} \tag{26}$$

Second, we fix $\boldsymbol{\alpha}$ to update $\boldsymbol{U}^{(i)}$ for all views. For $i$th view, we fix all $\boldsymbol{U}^{(l)}$ but $\boldsymbol{U}^{(i)}$. Maximizing Equation 22 can be transformed as the following equation:

$$\begin{aligned} &\max \quad \Omega(\boldsymbol{U}^{(i)}) = \alpha_i^r Tr\{(\boldsymbol{U}^{(i)})^T \boldsymbol{K}^{(i)} \boldsymbol{P}^{(i)} \boldsymbol{K}^{(i)} \boldsymbol{U}^{(i)}\} \\ &+ \sum_{v \neq l} \beta(N-1)^2 (\alpha_i^r + \alpha_l^r) Tr\{(\boldsymbol{U}^{(i)})^T \boldsymbol{K}^{(i)} \boldsymbol{G}^{(l)} (\boldsymbol{K}^{(i)})^T \boldsymbol{U}^{(i)}\} \\ &= Tr\{(\boldsymbol{U}^{(i)})^T \{\alpha_i^r \boldsymbol{K}^{(i)} \boldsymbol{P}^{(i)} \boldsymbol{K}^{(i)} + \sum_{v \neq l} (N-1)^2 \beta (\alpha_i^r + \alpha_l^r) \boldsymbol{K}^{(i)} \boldsymbol{G}^{(l)} (\boldsymbol{K}^{(i)})\} \boldsymbol{U}^{(i)}\} \\ &s.t. \quad (\boldsymbol{U}^{(i)})^T \boldsymbol{K}^{(i)} \boldsymbol{K}^{(i)} \ \boldsymbol{U}^{(i)} = \boldsymbol{I} \end{aligned} \tag{27}$$

Therefore, with the constraint $(\boldsymbol{U}^{(i)})^T \boldsymbol{K}^{(i)} \boldsymbol{K}^{(i)} \boldsymbol{U}^{(i)} = \boldsymbol{I}$, the optimizing $\boldsymbol{U}^{(i)}$ can be solved by eigenvectors which corresponds to the largest $d$ eigenvalues. Other $\boldsymbol{U}^{(l)}$s can also be solved by above procedure for updating themselves.

## 5 Experiment

In this section, we conduct experiments on 6 datasets to evaluate the performance of MSmPP by comparing with some DR methods.

### 5.1 Datasets

6 datasets are utilized in our experiments, including MSRC-v1, Caltech101, ORL, Extended Yale Face B, Cora, 3Sources, which are popular datasets used in literatures for evaluating DR methods. Among these datasets, Cora and 3Sources are multi-view text dataset. ORL, Extended Yale Face B and Caltech101 are image datasets, Figure 1, Figure 2, Figure 3and Figure 4 show some image samples of these image datasets.

MSRC-v1 dataset contains 240 images in 8 classes as a whole. We follow [37] to refine the data set, getting 7 classes composed of airplane, bicycle,building, cow, car, door, tree and each refined class has 30 images. Caltech 101 is an image dataset which contains 9144 images corresponding to 102 objects. For these two datasets, we extract features of the images from 4 views: GIST, LBP (local binary patterns), EDH (edge direction histogram), SIFT. ORL and Extended Yale Face B are 2 famous face image datasets. Extended Yale Face B consists of $192 \times 168$ pixels cropped face images,

Figure 1: Some examples of MSRC-v1.

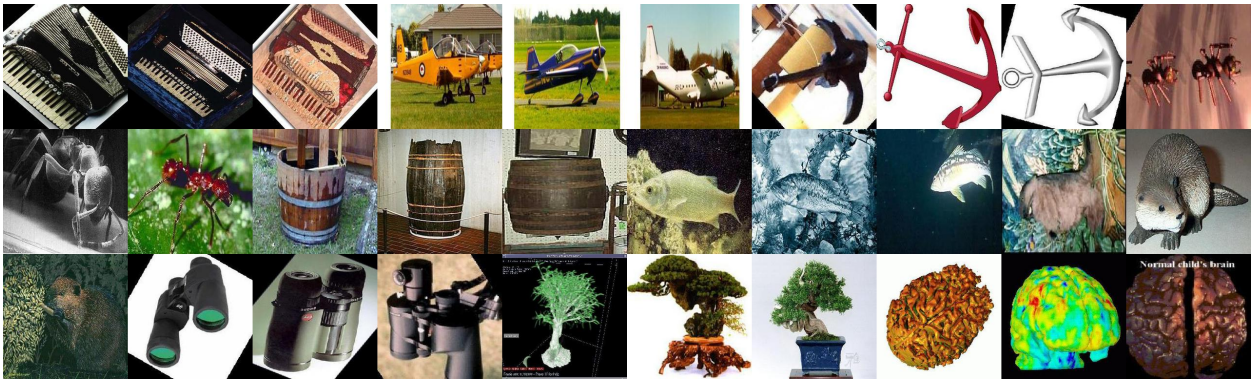


Figure 2: Some examples of Caltech101.

from 28 human subjects. ORL contains 10 different images of each of 40 distinct subjects for a total of 400 images. For these two datasets, we extract features utilizing gray-scale intensity, LBP, EDH. 3Sources is a multi-view text dataset, which is collected from three well-known online news sources: BBC, Reuters, and The Guardian. We select the 169 articles, which were reported in all three sources. Each source was treated as a view. Cora contains 2708 documents over the 7 labels. It is made of 4 views (content, inbound, outbound, cites) on the same documents.

We compare our MSmPP with 6 DR methods: 1. PCA, 2. SPP, 3. LPP, 4. NPE, 5. CCA, 6. NPE, 7. Our method1 (SmPP), 8. SmPP_CON 9. Our method2 (MSmPP). For those single view DR methods, we select the performances from the best single view and SmPP_CON represents SmPP with features concatenation.

### 5.2 Experimental Results

In this section, we conduct the experiments on 5 datasets. Firstly, we construct the optimal subspaces based on every DR methods with exploring the same training set. Then the 3NN classifier is utilized to classify all test samples to verify the performance of the methods. The Gaussian kernel is utilized in MSmPP. The $0-1$ weighted $k-$nn graph with $k=5$ is utilized in SmPP. A default value of regularization $\beta$ in Equation 22 is $0.25$.

For 3Sources dataset, we select 120 samples randomly as the training set. With the given training set, a 50-dimension subspace is learned by all methods respectively. Then, the test samples are transformed to the subspace by the learned projection matrix. In this experiment, 20 training/test splits are randomly generated and the average classification accuracies are shown in Table 1.

Figure 3: Some examples of ORL.

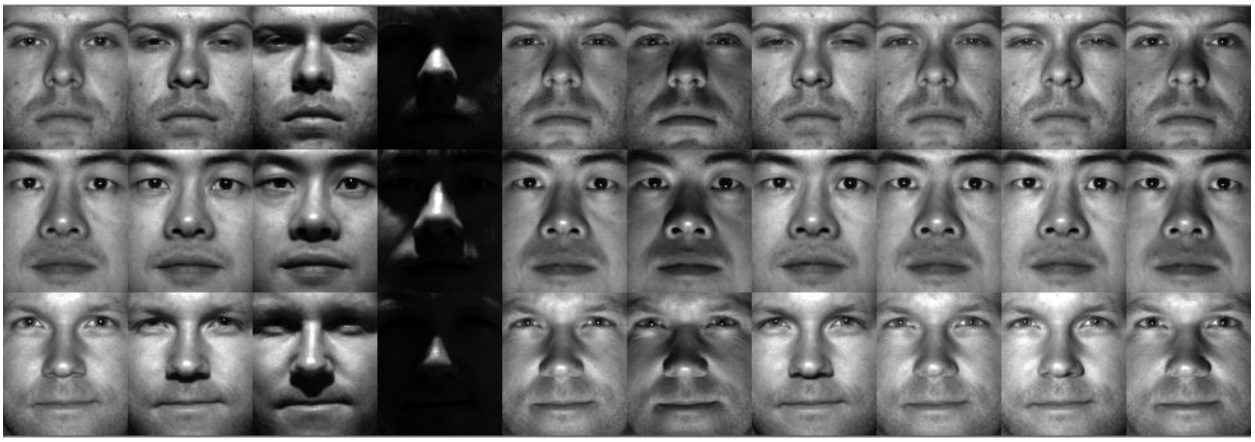

Figure 4: Some examples of YaleB.

Table 1: Classification results on 3Sources and Cora datasets.

| Method | 3Sources | | | Cora | | |
|---|---|---|---|---|---|---|
| | Min | Mean | Max | Min | Mean | Max |
| PCA | 63.17 | 74.86 | 80.62 | 40.28 | 43.10 | 45.31 |
| NPE | 60.39 | 63.65 | 70.38 | 40.09 | 46.72 | 52.86 |
| LPP | 60.70 | 72.23 | 79.98 | 34.43 | 38.22 | 50.21 |
| SPP | 62.08 | 75.22 | 79.39 | 39.21 | 44.34 | 49.88 |
| MCCA | 74.88 | 80.00 | 86.83 | 40.28 | 43.10 | 45.33 |
| SmPP | 73.22 | 81.42 | 87.79 | 42.83 | 44.11 | 48.50 |
| SmPP_CON | 62.17 | 78.61 | 82.32 | 39.28 | 41.16 | 48.62 |
| MSmPP | **78.58** | **83.22** | **93.31** | **46.28** | **57.21** | **66.96** |

For Cora dataset, we select 60% of samples per class as the training set. With the given training set, a 50-dimension subspace is learned by all methods respectively. Then, the test samples are transformed to the subspace by the learned projection matrix. In this experiment, 20 training/test splits are randomly generated and the average classification accuracies are in Table 1.

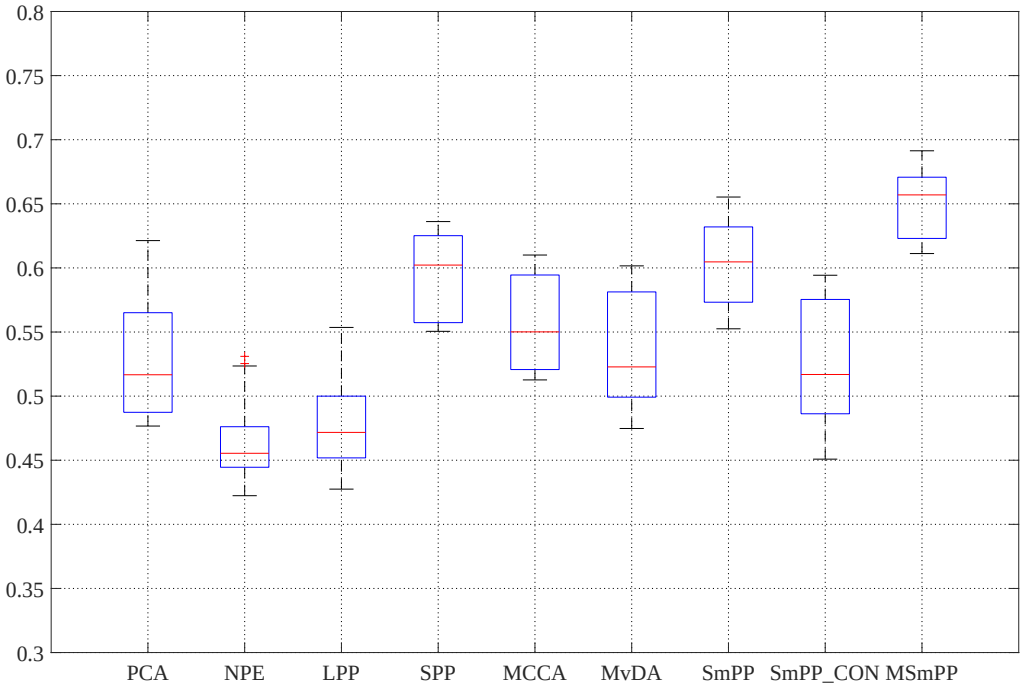


Figure 5: Classification results on YaleB dataset.

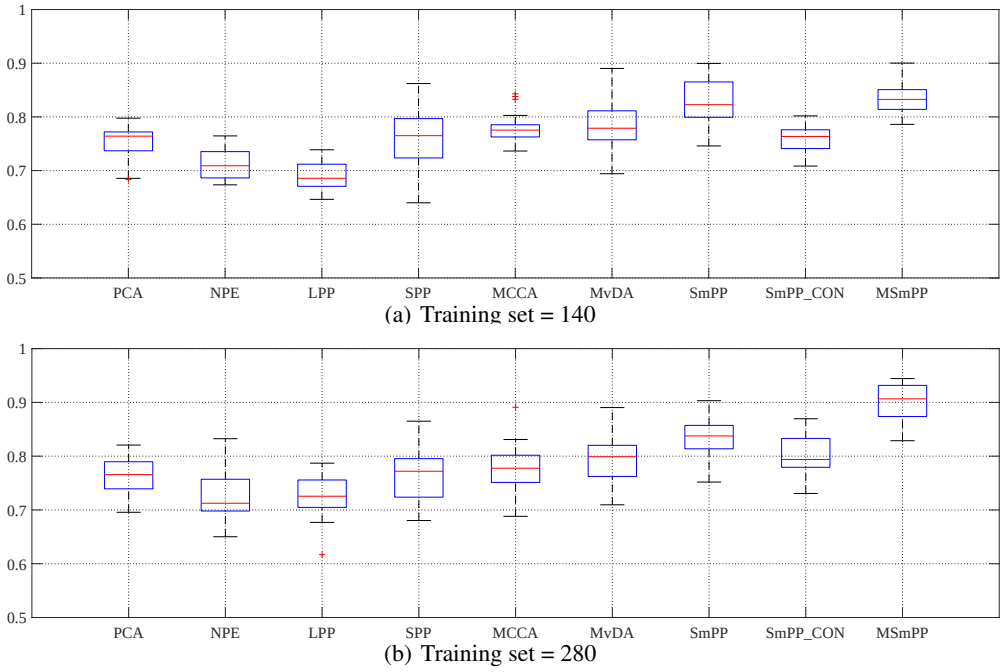


Figure 6: Classification results on MSRC-v1 dataset with different training numbers.

For the Extended Yale Face B dataset, we extract the features of the images from 3 views: gray-scale intensity, EDH, LBP. We utilize 20 classes of the dataset. Then we randomly select half of the images per class as the training set. With the given training set, a 30-dimension subspace is learned by all methods respectively. Then, the test samples are

transformed to the subspace by the learned projection matrix. In this experiment, 20 training/test splits are randomly generated and the average classification accuracies are in Figure 5.

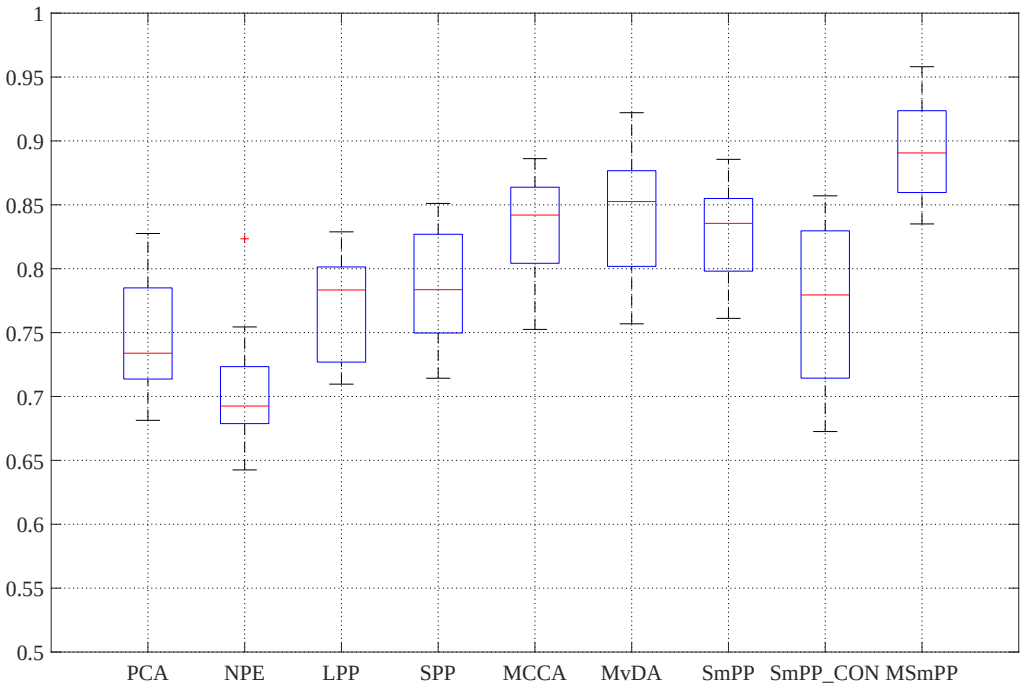


Figure 7: Classification results on ORL dataset.

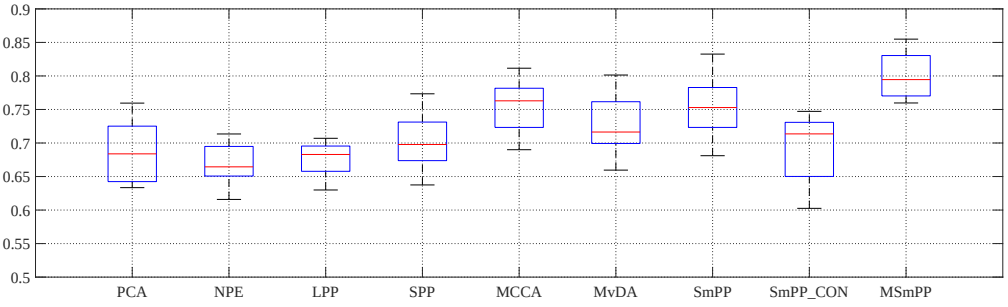


(a) Training set = 150

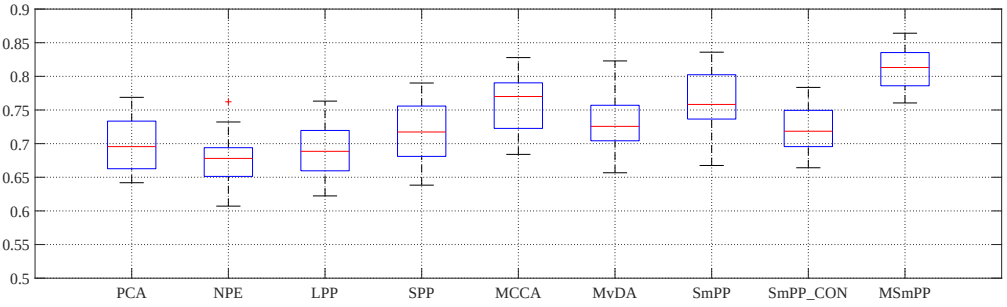


(b) Training set = 300

Figure 8: Classification results on Caltech101 dataset with different training numbers.

For ORL dataset, we utilize the same multi-view features as Yale Face B. 200 samples are randomly selected as training set. A 30-dimension subspace is learned by all methods respectively based on the given training set. Then, the test

samples are transformed to the subspace by the learned projection matrix. In this experiment, 20 training/test splits are randomly generated and the average classification accuracies are in Figure 7.

For the Extended Yale Face B dataset, we extract the features of the images from 3 views: gray-scale intensity, EDH, LBP. We utilize 20 classes of the dataset. Then we randomly select half of the images per class as the training set. With the given training set, a 30-dimension subspace is learned by all methods respectively. Then, the test samples are transformed to the subspace by the learned projection matrix. In this experiment, 20 training/test splits are randomly generated and the average classification accuracy are in Figure 5.

For Caltech 101 dataset, we extract the features of the images same with above. We utilize 15 classes of Caltech 101 in our experiments. Then we randomly select half of the images per class as the training set. With the given training set, a 70-dimension subspace is learned by all methods respectively. Then, the test samples are transformed to the subspace by the learned projection matrix. In this experiment, 20 training/test splits are randomly generated and the average classification accuracies are in Figure 8.

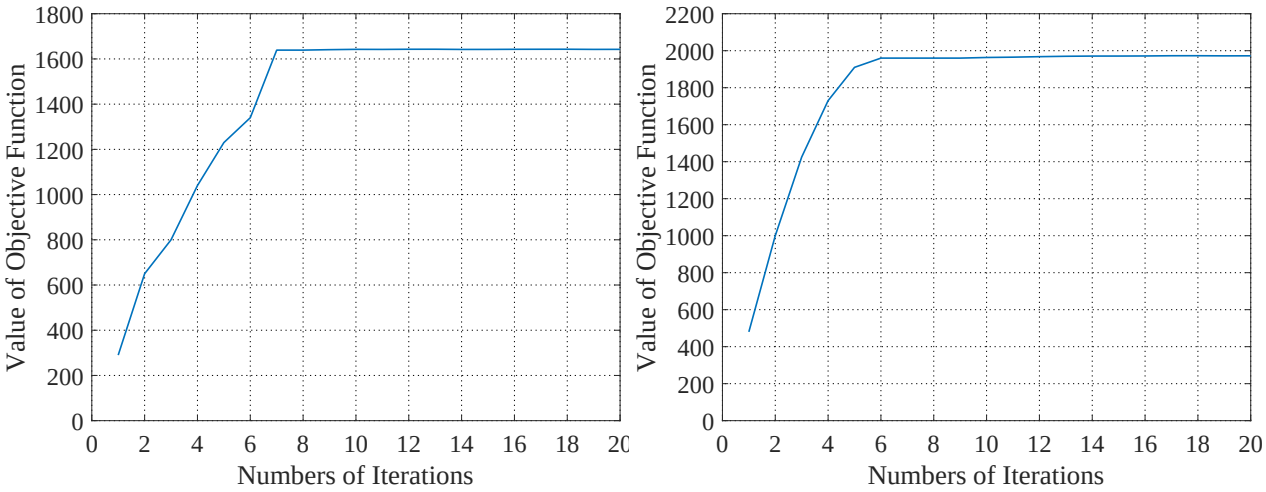


(a) Yale B (b) ORL

Figure 9: Objective values and Iterations on Yale B and ORL two datasets.

For MSRC-v1 dataset, we extract the features of the images same with above. We utilize 7 classes of MSRC-v1 in our experiments. We randomly select some images per class as the training set. With the given training set, a 70-dimension subspace is learned by all methods respectively. Then, the test samples are transformed to the subspace by the learned projection matrix. In this experiment, 20 training/test splits are randomly generated and the average classification accuracies are in Figure 12.

As can be seen, MSmPP outperforms the other DR methods. The single view SmPP, also has an excellent performance in the experiment. Since single SmPP only utilizes one single view, which can not get a fully integrate compatible and complementary information from multi-view features, SmPP can not outperform the MSmPP. Meanwhile, SmPP_CON concatenates features from all views and can not outperforms MSmPP, which verifies that the MSmPP has a more effective framework to integrate the information of the features from multiple views.

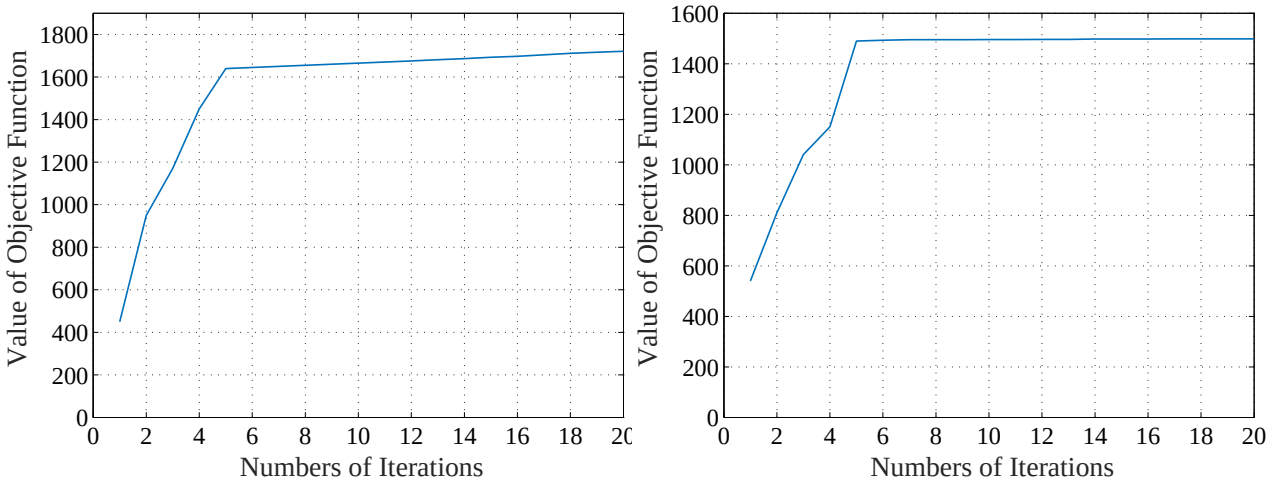


(a) Caltech101 (b) MSRC-v1

Figure 10: Objective values and Iterations on two datasets.

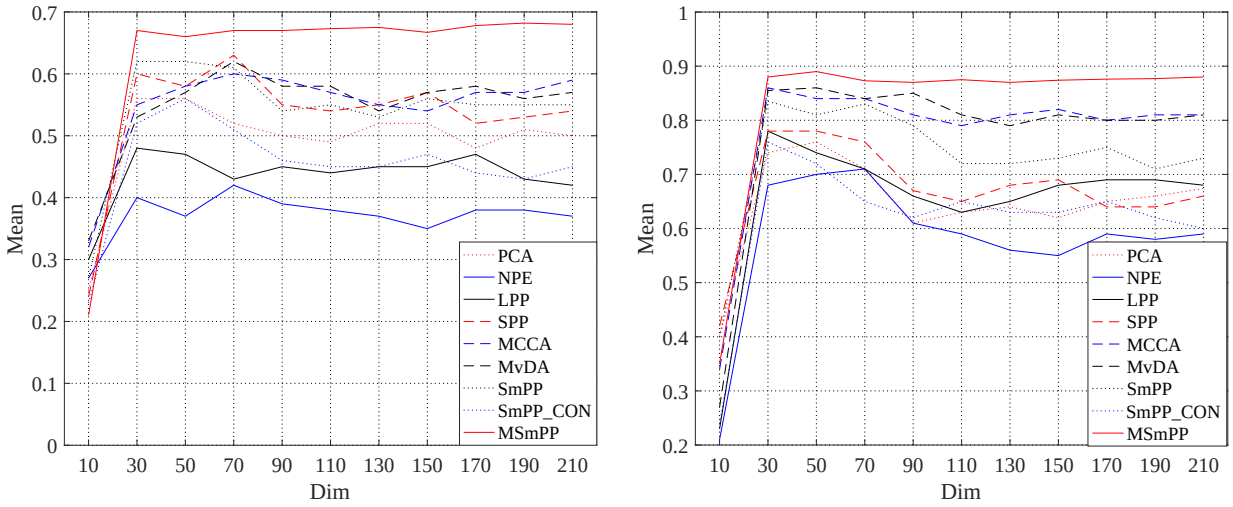


(a) YaleB (b) ORL

Figure 11: Classification results on Yale B and ORL datasets with different dimension.

## 6 Conclusion

In this paper, we propose a novel multi-view dimensional reduction method named Multi-view Smooth Preserving Projection. We first construct the single view DR method named SmPP, which computes the projection by preserving the smooth reconstructive weight as much as possible. Then, we extend the single view SmPP to multi-view version MSmPP. MSmPP fully exploits and preserves the smooth reconstructive weight between features from multiple views. The co-regularization scheme helps MSmPP to integrates the compatible and complementary information of multi-view features. The experiments testify to the advantage of MSmPP over many DR methods.

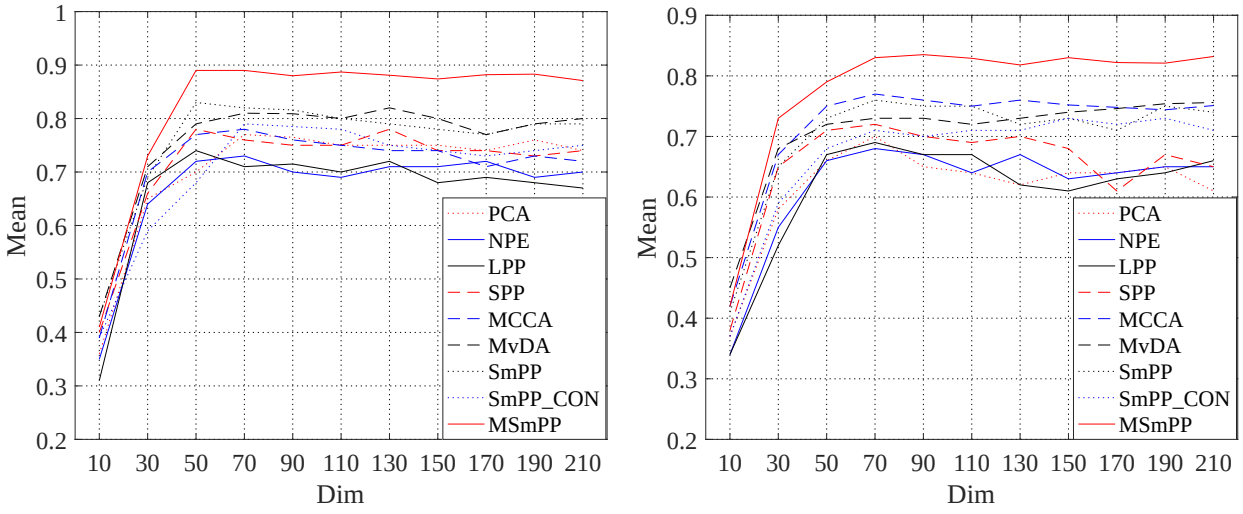


(a) MSRC-v1 (b) Caltech101

Figure 12: Classification results on MSRC-v1 and Caltech101 datasets with different dimension.

## Appendix

**Proof:**

Firstly, we reformulate Equation 8 as:

$$\min_{\boldsymbol{Z}} \eta|| \bar{\boldsymbol{X}} - \bar{\boldsymbol{X}}\boldsymbol{Z}||_F^2 + Tr(\boldsymbol{Z}\hat{\boldsymbol{L}}\boldsymbol{Z}^T). \tag{28}$$

The $\bar{\boldsymbol{x}_i} = [\boldsymbol{x}_i^T, 1]^T$ and $\bar{\boldsymbol{X}} = [\boldsymbol{X}^T, \boldsymbol{I}]^T$. The SMR model for $\bar{X}$ is as:

$$\min_{\boldsymbol{Z}} \eta||\bar{\boldsymbol{X}} - \bar{\boldsymbol{X}}\boldsymbol{Z}||_F^2 + Tr(\boldsymbol{Z}(\bar{\boldsymbol{L}} + \epsilon\boldsymbol{I})\boldsymbol{Z}^T) \tag{29}$$

where $\bar{\boldsymbol{L}}$ is the Laplace matrix of $\bar{\boldsymbol{X}}$. On the other hand, since Laplace matrix $\boldsymbol{L}$ is constructed based on the distance between two samples and $||\boldsymbol{x}_i - \boldsymbol{x}_j||_2 = ||\bar{\boldsymbol{x}_i} - \bar{\boldsymbol{x}_j}||_2$, the Laplace matrix $\bar{\boldsymbol{L}}$ of $\bar{\boldsymbol{X}}$ is same with the Laplace matrix $\boldsymbol{L}$ of $\boldsymbol{X}$. Therefore, the SMR model for $\bar{\boldsymbol{X}}$ can be expressed as Equation 28 and the optimal solution of Equation 28 has the grouping effect for $X$ that $||\boldsymbol{x}_i - \boldsymbol{x}_j||_2 \to 0 \Leftrightarrow ||\bar{\boldsymbol{x}_i} - \bar{\boldsymbol{x}_j}||_2 \to 0 \Rightarrow ||\boldsymbol{z}_i - \boldsymbol{z}_j||_2 \to 0$. The optimization procedure of Equation 29 is same to [35]. The optimal solution $Z$ satisfies $\sum_{j=1}^{n} z_{ij} = 1$ without requirement of normalization, when $alpha$ is large enough ($\eta > 0.2$, empirically).

Meanwhile, the objective function Equation 28 also satisfies EGE conditions [35]. Equation 6 is a smooth convex program. Therefore, the optimal solution $Z^*$ of the objective function can be computed by differentiating the function respect to $Z$ and setting it to 0.

$$\alpha X^T X Z^\star + Z^\star \hat{L} = \alpha X^T X. \tag{30}$$

Equation 28 is a standard Sylvester equation [38], which has a unique solution.

## References

[1] Shiliang Sun. A survey of multi-view machine learning. *Neural Computing & Applications*, 23(7-8):2031–2038, 2013.

[2] Yingming Li, Ming Yang, and Zhongfei Mark Zhang. A survey of multi-view representation learning. *IEEE Transactions on Knowledge and Data Engineering*, 2018.

[3] Zhao Jing, Xijiong Xie, Xu Xin, and Shiliang Sun. Multi-view learning overview: Recent progress and new challenges. *Information Fusion*, 38:43–54, 2017.

[4] F. Nie, G. Cai, J. Li, and X. Li. Auto-weighted multi-view learning for image clustering and semi-supervised classification. *IEEE Transactions on Image Processing*, 27(3):1501–1511, March 2018.

[5] S Wold. Principal component analysis. *Chemometrics & Intelligent Laboratory Systems*, 2(1):37–52, 1987.

[6] Suresh Balakrishnama and Aravind Ganapathiraju. Linear discriminant analysis-a brief tutorial. *Institute for Signal and information Processing*, 18:1–8, 1998.

[7] Xiaofei He and Partha Niyogi. Locality preserving projections. In *Advances in neural information processing systems*, pages 153–160, 2004.

[8] Xiaofei He, Deng Cai, Shuicheng Yan, and Hong-Jiang Zhang. Neighborhood preserving embedding. In *Tenth IEEE International Conference on Computer Vision (ICCV'05) Volume 1*, volume 2, pages 1208–1213. IEEE, 2005.

[9] Dong Xu, Shuicheng Yan, Dacheng Tao, Stephen Lin, and Hong-Jiang Zhang. Marginal fisher analysis and its variants for human gait recognition and content-based image retrieval. *IEEE Transactions on Image processing*, 16(11):2811–2821, 2007.

[10] Deng Cai, Xiaofei He, Kun Zhou, Jiawei Han, and Hujun Bao. Locality sensitive discriminant analysis. In *IJCAI*, volume 2007, pages 1713–1726, 2007.

[11] Zhenyue Zhang and Hongyuan Zha. Principal manifolds and nonlinear dimensionality reduction via tangent space alignment. *Journal of Shanghai University (English Edition)*, 8(4):406–424, 2004.

[12] Jie Gui, Zhenan Sun, Jia Wei, Rongxiang Hu, Yingke Lei, and Shuiwang Ji. Discriminant sparse neighborhood preserving embedding for face recognition. *Pattern Recognition*, 45(8):2884–2893, 2012.

[13] Lin Feng, Huibing Wang, Shenglan Liu, and Hongwei Zhang. Locality structured sparsity preserving embedding. *International Journal of Pattern Recognition & Artificial Intelligence*, 29(6):150621203409007, 2015.

[14] Lishan Qiao, Songcan Chen, and Xiaoyang Tan. Sparsity preserving projections with applications to face recognition. *Pattern Recognition*, 43(1):331–341, 2010.

[15] Sam T Roweis and Lawrence K Saul. Nonlinear dimensionality reduction by locally linear embedding. *science*, 290(5500):2323–2326, 2000.

[16] Mikhail Belkin and Partha Niyogi. Laplacian eigenmaps for dimensionality reduction and data representation. *Neural computation*, 15(6):1373–1396, 2003.

[17] D. R. Hardoon, S Szedmak, and J Shawetaylor. Canonical correlation analysis: an overview with application to learning methods. *Neural Computation*, 16(12):2639–2664, 2004.

[18] Meina Kan, Shiguang Shan, Haihong Zhang, Shihong Lao, and Xilin Chen. Multi-view discriminant analysis. In *European Conference on Computer Vision*, pages 188–194, 2012.

[19] Tian Xia, Dacheng Tao, Tao Mei, and Yongdong Zhang. Multiview spectral embedding. *IEEE Transactions on Systems, Man, and Cybernetics, Part B (Cybernetics)*, 40(6):1438–1446, 2010.

[20] Z. Ding and Y. Fu. Low-rank common subspace for multi-view learning. In *2014 IEEE International Conference on Data Mining*, pages 110–119, Dec 2014.

[21] C. Xu, D. Tao, and C. Xu. Multi-view learning with incomplete views. *IEEE Transactions on Image Processing*, 24(12):5812–5825, Dec 2015.

[22] Hao Zheng, Xin Geng, Dacheng Tao, and Zhong Jin. A multi-task model for simultaneous face identification and facial expression recognition. *Neurocomputing*, 171(C):S0925231215010097, 2016.

[23] Chang Xu, Dacheng Tao, and Chao Xu. Multi-view intact space learning. *IEEE transactions on pattern analysis and machine intelligence*, 37(12):2531–2544, 2015.

[24] Y Wang, Z Wenjie, L Wu, X Lin, M Fang, and S Pan. Iterative views agreement: An iterative low-rank based structured optimization method to multi-view spectral clustering. In *IJCAI International Joint Conference on Artificial Intelligence*, pages 2153–2159, 2016.

[25] Y. Wang, X. Lin, L. Wu, W. Zhang, Q. Zhang, and X. Huang. Robust subspace clustering for multi-view data by exploiting correlation consensus. *IEEE Transactions on Image Processing*, 24(11):3939–3949, Nov 2015.

[26] Y. Wang, L. Wu, X. Lin, and J. Gao. Multiview spectral clustering via structured low-rank matrix factorization. *IEEE Transactions on Neural Networks and Learning Systems*, 29(10):4833–4843, Oct 2018.

[27] Y. Wang, X. Lin, L. Wu, and W. Zhang. Effective multi-query expansions: Collaborative deep networks for robust landmark retrieval. *IEEE Transactions on Image Processing*, 26(3):1393–1404, March 2017.

[28] L. Wu, Y. Wang, and L. Shao. Cycle-consistent deep generative hashing for cross-modal retrieval. *IEEE Transactions on Image Processing*, 28(4):1602–1612, April 2019.

[29] L. Wu, Y. Wang, X. Li, and J. Gao. Deep attention-based spatially recursive networks for fine-grained visual recognition. *IEEE Transactions on Cybernetics*, 49(5):1791–1802, May 2019.

[30] L. Wu, Y. Wang, J. Gao, and X. Li. Where-and-when to look: Deep siamese attention networks for video-based person re-identification. *IEEE Transactions on Multimedia*, 21(6):1412–1424, June 2019.

[31] Yang Wang and Lin Wu. Beyond low-rank representations: Orthogonal clustering basis reconstruction with optimized graph structure for multi-view spectral clusering. *Neural Networks*, 103:1 – 8, 2018.

[32] Jun Yu, Dacheng Tao, Yong Rui, and Jun Cheng. Pairwise constraints based multiview features fusion for scene classification. *Pattern Recognition*, 46(2):483 – 496, 2013.

[33] Canyi Lu, Jiashi Feng, Zhouchen Lin, and Shuicheng Yan. Correlation adaptive subspace segmentation by trace lasso. *CoRR*, abs/1501.04276, 2015.

[34] Can-Yi Lu, Hai Min, Zhong-Qiu Zhao, Lin Zhu, De-Shuang Huang, and Shuicheng Yan. Robust and efficient subspace segmentation via least squares regression. *CoRR*, abs/1404.6736, 2014.

[35] Han Hu, Zhouchen Lin, Jianjiang Feng, and Jie Zhou. Smooth representation clustering. In *Proceedings of the IEEE Conference on Computer Vision and Pattern Recognition*, pages 3834–3841, 2014.

[36] Sebastian Mika, Alex Smola, and Matthias Scholz. Kernel pca and de-noising in feature spaces. In *Conference on Advances in Neural Information Processing Systems II*, 1999.

[37] X. Cai, F. Nie, H. Huang, and F. Kamangar. Heterogeneous image feature integration via multi-modal spectral clustering. In *CVPR 2011*, pages 1977–1984, June 2011.

[38] Richard H. Bartels and G. W. Stewart. Solution of the matrix equation ax+xb=c [f4] (algorithm 432). *Communications of the Acm*, 15(9):820–826, 1972.